



Since January 2020 Elsevier has created a COVID-19 resource centre with free information in English and Mandarin on the novel coronavirus COVID-19. The COVID-19 resource centre is hosted on Elsevier Connect, the company's public news and information website.

Elsevier hereby grants permission to make all its COVID-19-related research that is available on the COVID-19 resource centre - including this research content - immediately available in PubMed Central and other publicly funded repositories, such as the WHO COVID database with rights for unrestricted research re-use and analyses in any form or by any means with acknowledgement of the original source. These permissions are granted for free by Elsevier for as long as the COVID-19 resource centre remains active.



SARS-CoV-2 in cardiac tissue of a child with COVID-19-related multisystem inflammatory syndrome

Marisa Dolhnikoff*, Juliana Ferreira Ferranti*, Renata Aparecida de Almeida Monteiro, Amaro Nunes Duarte-Neto, Michele Soares Gomes-Gouvêa, Natália Viu Degaspere, Artur Figueiredo Delgado, Carolina Montanari Fiorita, Gabriela Nunes Leal, Regina Maria Rodrigues, Khallil Taverna Chaim, João Renato Rebello Pinho, Magda Carneiro-Sampaio, Thais Mauad, Luiz Fernando Ferraz da Silva, Werther Brunow de Carvalho, Paulo Hilario Nascimento Saldiva, Elia Garcia Caldini

Lancet Child Adolesc Health
2020; 4: 790–94

Published Online
August 20, 2020

[https://doi.org/10.1016/S2352-4642\(20\)30257-1](https://doi.org/10.1016/S2352-4642(20)30257-1)

This online publication has been corrected. The corrected version first appeared at thelancet.com/child-adolescent on Sept 16, 2020

*Contributed equally

Departamento de Patologia

(M Dolhnikoff MD,

RA de Almeida Monteiro MD,

A N Duarte-Neto MD,

K Taverna Chaim MSc,

T Mauad MD,

L F Ferraz da Silva MD,

Prof P H N Saldiva MD,

E Garcia Caldini PhD), Instituto

da Criança

(J Ferreira Ferranti MD,

N Viu Degaspere MD,

A Figueiredo Delgado MD,

C Montanari Fiorita MD,

G Nunes Leal MD,

R M Rodrigues MD,

Prof M Carneiro-Sampaio MD,

Prof W Brunow de Carvalho MD),

and Departamento de

Gastroenterologia

(M Soares Gomes-Gouvêa PhD,

J R Rebello Pinho MD),

Faculdade de Medicina da

Universidade de São Paulo,

São Paulo, Brazil; and Serviço

de Verificação de Óbitos da

Capital, Universidade de

São Paulo, São Paulo, Brazil

(L F Ferraz da Silva)

Correspondence to:

Dr Marisa Dolhnikoff, Faculdade

de Medicina da Universidade de

São Paulo, Departamento de

Patologia, Sao Paulo 01246-903,

Brazil

maridol@usp.br

We report the case of an 11-year-old child with multi-system inflammatory syndrome in children (MIS-C) related to COVID-19 who developed cardiac failure and died after 1 day of admission to hospital for treatment. An otherwise healthy female of African descent, the patient was admitted to the paediatric intensive care unit (ICU) with cardiovascular shock and persistent fever. Her initial symptoms were fever for 7 days, odynophagia, myalgia, and abdominal pain. On admission to the ICU, the patient presented with respiratory distress, comprising tachypnoea (respiratory rate 70 breaths per min) and hypoxia, and signs of congestive heart failure, including jugular vein

distention, crackles at the base of the lungs, displaced liver, hypotension (blood pressure 80/36 mm Hg), tachycardia (134 beats per min [bpm]), and cold extremities with filiform pulses. Non-exudative conjunctivitis and cracked lips were present on physical examination. The patient was promptly intubated and antibiotic treatment was started with ceftriaxone and azithromycin. Peripheral epinephrine was initiated in the emergency room before the patient was moved to paediatric ICU.

A point-of-care echocardiogram showed diffuse left-ventricular hypokinesia with no segmental wall motion abnormalities. Left-ventricular ejection fraction was

	0 h	7 h	14 h	17 h	24 h	Normal range
Haemoglobin, g/dL	10.0	11.8	12.1	11.4	11.0	12.7–14.7
Hematocrit, %	28.8%	34.3%	36.4%	34.3%	33.0%	38.0–44.0%
Platelets, $\times 10^3$ cells per μ L	167	..	191	..	145	150–450
White blood cell count, $\times 10^3$ cells per mm^3	25.73	24.28	35.90	40.30	38.22	4.50–14.40
Lymphocytes, %	1.03%	0.73%	0.36%	0.40%	3.44%	38.00–42.00%
Urea, mg/dL	67	73	78	78	93	11–38
Creatinine, mg/dL	1.27	1.31	1.56	1.73	2.19	0.53–0.79
D-dimer, ng/mL	11 495	..	54 153	<500
Troponin, ng/mL	0.281	..	0.290	0.342	..	<0.014
Creatine kinase myocardial band, ng/mL	5.76	..	28.50	15.66	..	0.10–2.88
Interleukin-6, pg/mL	4105.0	0.2–7.8
Creatine kinase, U/L	96	<167
Blood pH	7.21	7.30	..	7.28	7.31	7.35–7.45
Bicarbonate, mEq/L	15.7	16.4	..	17.6	17.2	21.0–28.0
PaCO ₂ , mm Hg	41	32	..	31	..	35–45
PaO ₂ , mm Hg	60	270	..	133	..	80–90
ScvO ₂ , %	87.2%	97.3%	..	82.0%	82.2%	60.0–85.0%
Lactate, mg/dL	38.0	39.0	..	27.0	..	4.5–14.4
C-reactive protein, mg/L	266.6	..	309.5	<5.0
Total protein, g/dL	5.0	6.0–8.0
Albumin, g/dL	2.6	3.8–5.4
Aspartate aminotransferase, U/L	61	..	67	13–35
Alanine aminotransferase, U/L	67	..	67	7–35
Oxygenation index	..	3.1	..	4.2	..	<4.0
International normalised ratio	1.4	0.9–1.2
Fibrinogen, mg/dL	513	200–393
Ferritin, ng/mL	1501	..	20–200
Triglycerides, mg/dL	162	..	<100

PaCO₂=partial pressure of carbon dioxide in arterial blood. PaO₂=partial pressure of oxygen in arterial blood. ScvO₂=central venous saturation of oxygen.

Table: Laboratory results at various timepoints after presentation

estimated with the M-mode Teichholz method in the parasternal short axis view, at the level of the papillary muscles of the mitral valve; substantial myocardial dysfunction was noted, with decreased left-ventricular ejection fraction (31%) and no respiratory collapsibility of the inferior vena cava. The patient received furosemide, and central line and invasive arterial monitoring were established. Initial radiography showed an enlarged cardiac area and bilateral lung opacities (appendix p 1). Chest CT showed multiple ground-glass pulmonary opacities associated with thickening of interlobular septa and sparse bilateral foci of consolidation, predominantly in the peripheral and posterior areas of lower lobes (appendix p 1).

Laboratory results showed high concentrations of markers of systemic inflammation and myocardial injury, including C-reactive protein, interleukin-6, ferritin, triglycerides, D-dimer, troponin, and creatine kinase myocardial band. Moreover, a left-shifted white-blood-cell count and substantial lymphopenia were seen. Blood gas analysis showed hypoxia and acidosis (table).

Mechanical ventilation was implemented during the first hour in the ICU and ventilatory parameters reached a maximum positive end-expiratory pressure of 8 cm H₂O and peak inspiratory pressure of 25 cm H₂O, with an initial fraction of inspired oxygen of 60%. After initiation of mechanical ventilation and use of diuretics, ventilatory parameters could be reduced and less opacification was seen on chest radiography.

The patient had sinus tachycardia throughout the hospital stay (heart rate >200 bpm); the initial electrocardiogram is shown in figure 1. The patient progressed to hyperdynamic vasoplegic shock refractory to volume resuscitation and vasoactive agents. After 28 h of hospital admission, she developed ventricular fibrillation and died.

An ultrasound-guided minimally invasive autopsy was done, with tissue sampling of the heart, lungs, liver, spleen, kidneys, brain, inguinal lymph node, quadriceps muscle, and skin.¹ Post-mortem CT angiography was done before tissue collection and did not show any signs of coronary artery alterations (appendix p 2). Post-mortem ultrasound examination of the heart showed a hyperechogenic and diffusely thickened endocardium (mean thickness 10 mm), a thickened myocardium (18 mm thick in the left ventricle), and a small pericardial effusion. Histopathological examination showed myocarditis, pericarditis, and endocarditis characterised by inflammatory cell infiltration (figure 2A). Inflammation was mainly interstitial and perivascular, associated with foci of cardiomyocyte necrosis (figure 2B, C), and was mainly composed of CD68⁺ macrophages (figure 2E), a few CD45⁺ lymphocytes (figure 2F), and a few neutrophils and eosinophils. C4d immunostaining was used for detection of cardiomyocyte necrosis (figure 2D). Analysis of cardiac tissue by electron

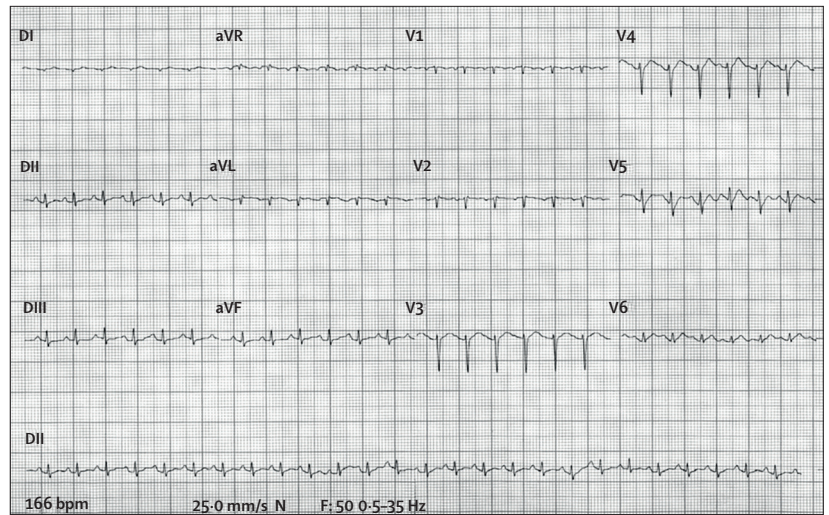


Figure 1: Electrocardiogram showing sinus tachycardia on admission

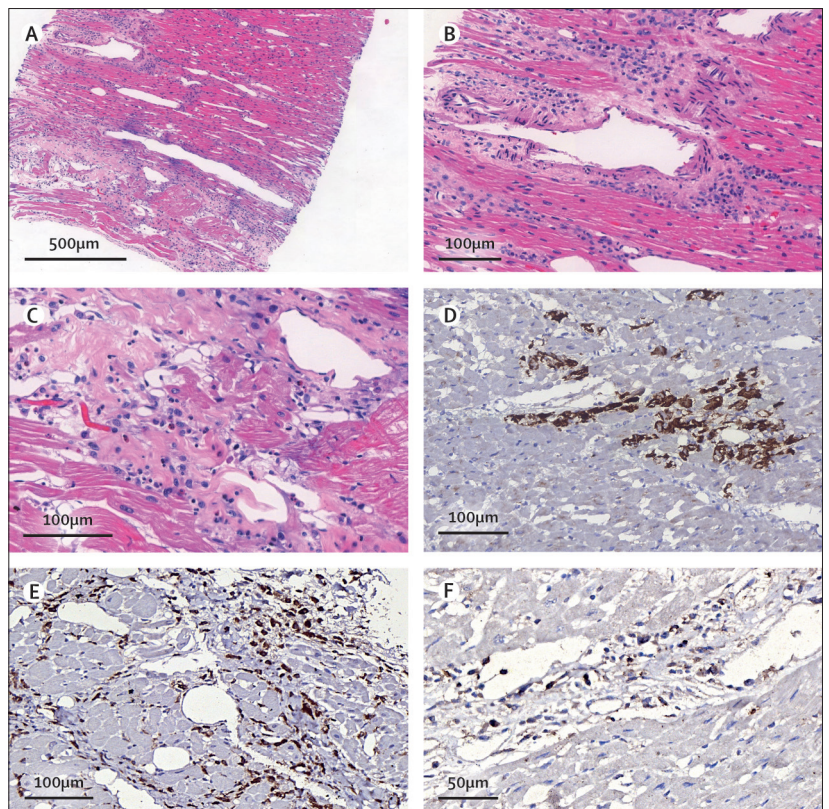


Figure 2: Post-mortem histological findings

(A) Diffuse myocardial interstitial inflammation. (B, C) Interstitial and perivascular myocardial inflammation containing lymphocytes, macrophages, a few neutrophils and eosinophils, and foci of cardiomyocyte necrosis. (D) Myocardial necrosis indicated by C4d staining. (E, F) Myocardial interstitial inflammation containing CD68⁺ (E) and CD45⁺ (F) cells.

microscopy identified spherical viral particles of 70–100 nm in diameter, consistent in size and shape with the Coronaviridae family, in the extracellular compartment and within several cell types—

See Online for appendix

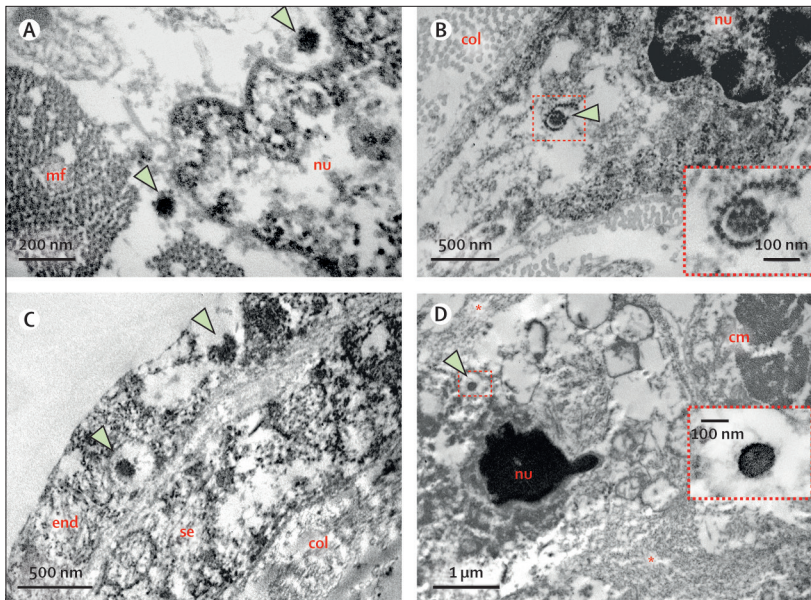


Figure 3: Post-mortem electron microscopy findings

(A) Part of a cardiomyocyte, with viral particles (arrows) within a cytoplasmic area close to the nucleus. (B) Part of a fibroblast; arrow points to a viral particle inside a ruptured fragment of the rough endoplasmic reticulum. Inset in (B) corresponds to a higher magnification of the virus. (C) Endothelial lining (endocardium and subendocardium) of the left ventricular lumen; two viral particles (arrows) are present inside the endothelial cell. (D) Neutrophil in late stages of NETosis; asterisks indicate neutrophil extracellular traps (decondensed and dispersed chromatin); arrow points to a viral particle inside a cytoplasmic vesicle. Inset in (D) shows the viral particle at high magnification. cm=cardiomyocyte. col=collagen fibrils. end=endothelial cell. mf=myofibrils. NET=neutrophil extracellular trap. nu=nucleus. se=subendocardial fibroblast.

For the **UCSC Genome Browser** see <http://genome.ucsc.edu>
For more on **Burrows-Wheeler Aligner** software see <http://bio-bwa.sourceforge.net/>

cardiomyocytes, capillary endothelial cells, endocardium endothelial cells, macrophages, neutrophils, and fibroblasts (figure 3). Microthrombi in the pulmonary arterioles (appendix p 3) and renal glomerular capillaries were also noted at autopsy. Severe acute respiratory syndrome coronavirus 2 (SARS-CoV-2)-associated pneumonia was mild, with patchy exudative changes in alveolar spaces and mild pneumocyte hyperplasia (appendix p 3). Lymphoid depletion and signs of haemophagocytosis were noted in the spleen and lymph nodes, indicating secondary haemophagocytic lymphohistiocytosis associated with systemic inflammation. Acute tubular necrosis in the kidneys and hepatic centrilobular necrosis, secondary to shock, were also seen. Brain tissue showed microglial reactivity.

SARS-CoV-2 RNA was detected on a post-mortem nasopharyngeal swab and in cardiac and pulmonary tissues by real time RT-PCR using primers and probes set for E (envelope) gene.² Cycle threshold values for lung and heart samples were 35.6 and 36.0, respectively, suggesting a low viral load in both organs.

To investigate a primary immunodeficiency, whole-exome sequencing from genomic DNA extracted from whole blood was done, using a customised Twist Human Core Exome kit (Twist Bioscience, San Francisco, CA, USA) for exon capture, and sequenced in an Illumina NovaSeq platform (Illumina, San Diego, CA, USA).

Sequence reads were aligned to the reference human genome (GrCh38/hg38 in the University of California Santa Cruz [UCSC] Genome Browser) with Burrows-Wheeler Aligner software. Genotyping was done using the Genome Analysis Toolkit (Broad Institute, Cambridge, MA, USA).³ No pathogenic, likely pathogenic, or variant of unknown significance was found associated with inborn errors of immunity.

MIS-C is a severe clinical condition that has been described in several paediatric patients diagnosed with COVID-19 and that might be associated with cardiac dysfunction.⁴⁻¹⁰ Since the disorder shares similarities with Kawasaki disease, it has also been reported as Kawasaki-like disease or Kawasaki-like multisystem inflammatory syndrome.⁴⁻⁸ A substantial increase in the incidence of Kawasaki-like disease has been described in several countries with high incidence of COVID-19.^{4,5,7} In Italy, the first European country to be affected by the COVID-19 pandemic, Verdoni and colleagues⁴ found that, over a period of 1 month, the spread of SARS-CoV-2 was associated with a 30-fold increase in the incidence of Kawasaki-like disease. Compared with classic Kawasaki disease, children with MIS-C are older, have respiratory, gastrointestinal, neurological, and cardiovascular involvement, substantial lymphopenia, thrombocytopenia, and markers of myocarditis.^{4,7,8} Although previous studies have reported low mortality among children with MIS-C (<2%), patients presented with cardiogenic shock, acute left-ventricular dysfunction, and signs of myocarditis, indicating a potential risk of a life-threatening condition.⁴⁻¹⁰ The mechanism of heart failure in these patients and its relation to SARS-CoV-2 infection is not understood.

Possible mechanisms involved in cardiac dysfunction in children with COVID-19 include myocardial stunning or oedema associated with a severe systemic inflammatory state, direct myocardial injury by SARS-CoV-2, and hypoxia secondary to viral pneumonia.⁴⁻¹¹ Reports of substantial numbers of children presenting with MIS-C or Kawasaki-like disease during the COVID-19 pandemic indicate that SARS-CoV-2 is probably a trigger of this clinical condition, either by eliciting a severe systemic immune response or by direct tissue damage, or both.⁴⁻¹⁰

Our case report shows inflammatory changes in the cardiac tissue of a child with MIS-C related to COVID-19, which led to cardiac failure and death. SARS-CoV-2 could be detected in cardiac tissue by RT-PCR and electron microscopy. Despite the evident systemic inflammation and final progression to multiorgan failure, clinical, echocardiographic, and laboratory findings strongly indicated that heart failure was the main determinant of the fatal outcome. Further, the autopsy showed myocarditis, pericarditis, and endocarditis, with intense and diffuse tissue inflammation, and necrosis of cardiomyocytes. Moreover, the finding of SARS-CoV-2 in heart tissue indicates that myocardial inflammation was

probably a primary response to the virus-induced injury to cardiac cells. The presence of SARS-CoV-2 in different cell types of cardiac tissue suggests potential mechanisms for heart damage. First, infection of cardiomyocytes probably leads to local inflammation in response to cell injury; both the virus-induced injury and the inflammatory response could lead to necrosis of cardiomyocytes. The finding of viral particles in neutrophils supports the idea of virus-induced inflammation. Also, infection of endothelial cells in the endocardium could result in haematogenous spread of SARS-CoV-2 to other organs and tissues.

Detection of both SARS-CoV-2 RNA by RT-PCR and viral particles by electron microscopy in cardiac tissue has been reported in endomyocardial biopsy specimens from adults with COVID-19.^{12,13} Tavazzi and colleagues¹³ detected viral particles in cardiac macrophages in an adult patient with acute cardiac injury associated with COVID-19; no viral particles were seen in cardiomyocytes or endothelial cells. Our case report is the first to our knowledge to document the presence of viral particles in the cardiac tissue of a child affected by MIS-C. Moreover, viral particles were identified in different cell lineages of the heart, including cardiomyocytes, endothelial cells, mesenchymal cells, and inflammatory cells.

Two other reports in adolescents with COVID-19 detected myocarditis by MRI or at autopsy.^{14,15} In the report from Craven and colleagues,¹⁵ histological analysis of the heart of a 17-year-old boy showed diffuse myocarditis with mixed inflammatory infiltrate, with a predominance of eosinophils. In our case report, cardiac inflammation also included a small number of eosinophils. In these two previous reports,^{14,15} common symptoms of COVID-19 were absent, except for fever; pulmonary changes were absent or mild, and there was no multiorgan involvement.

The pulmonary involvement noted in our case report was probably the result of mild pneumonia, cardiogenic oedema, and microthrombi in the pulmonary arteriolar bed, which—associated with the finding of microthrombi in the kidney and the presence of virus in the cardiac capillary endothelium—suggest a SARS-CoV-2-induced endothelial dysfunction that probably involved several organs.

Whole-exome sequencing could not identify any inborn error of immunity in our patient. It is still unclear which host factors could predispose children to MIS-C; further investigation of potential genetic determinants is important to understand the pathogenesis of this syndrome.¹⁰

In conclusion, our pathological observations support the hypothesis that the direct effect of SARS-CoV-2 infection on cardiac tissue was a major contributor to myocarditis and heart failure in our patient. Hopefully, our findings could help to shed light on the understanding of the complex interaction between

SARS-CoV-2 infection, MIS-C, and cardiac dysfunction in children and adolescents with COVID-19.

Contributors

JFF, NVD, AFD, CMF, GNL, RMR, MCS, and WBdC were involved in the care of the patient. MD, RAdAM, AND-N, TM, LFFdS, and PHNS obtained and interpreted autopsy data. KTC did post-mortem CT angiography and interpreted these data. MSG-G and JRRP did molecular analyses and interpreted these data. EGC did electron microscopy and interpreted these data. MD and JFF wrote the report, and all authors reviewed and approved the final version.

Declaration of interests

We declare no competing interests.

Acknowledgments

This work was approved by the Hospital das Clínicas da Faculdade de Medicina da Universidade de São Paulo (HC-FMUSP) ethics committee (protocol no 3951.904) and written informed consent for publication was obtained from the patient's parent. We thank Jair Theodoro Filho, Kely Cristina Soares Bispo, Reginaldo Silva do Nascimento, Thabata Larissa Luciano Ferreira Leite, Catia Sales de Moura, and Marcelo Alves Ferreira for technical support; Luiz Alberto Benvenuti (Instituto do Coração, HC-FMUSP) for immunohistochemical staining and suggestions on histopathological analysis; Leila Antonangelo and Caroline Silverio Faria (Laboratório de Investigação Médica - 03, HC-FMUSP) for the cytokine profile analysis; and all workers involved in care for patients with COVID-19 and who are part of the HC-FMUSP Coronavirus Crisis Committee. This work was funded by Fundação de Amparo à Pesquisa do Estado de São Paulo (2013/17159-2, 2014/50489-9), Bill & Melinda Gates Foundation (INV-002396), and Conselho Nacional de Desenvolvimento Científico e Tecnológico (304987/2017-4). The funders had no role in study design, data collection, data analysis, data interpretation, or writing of the report. The corresponding author had full access to all data in the study and had final responsibility for the decision to submit for publication.

References

- Nunes Duarte-Neto A, de Almeida Monteiro RA, da Silva LFF, et al. Pulmonary and systemic involvement of COVID-19 assessed by ultrasound-guided minimally invasive autopsy. *Histopathology* 2020; published online May 22. <https://doi.org/10.1111/his.14160>.
- Corman VM, Landt O, Kaiser M, et al. Detection of 2019 novel coronavirus (2019-nCoV) by real-time RT-PCR. *Euro Surveill* 2020; 25: 2000045.
- Bousfiha A, Jeddane L, Picard C, et al. Human inborn errors of immunity: 2019 update of the IUIS phenotypical classification. *J Clin Immunol* 2020; 40: 66–81.
- Verdoni L, Mazza A, Gervasoni A, et al. An outbreak of severe Kawasaki-like disease at the Italian epicentre of the SARS-CoV-2 epidemic: an observational cohort study. *Lancet* 2020; 395: 1771–78.
- Ouldali N, Pouletty M, Mariani P, et al. Emergence of Kawasaki disease related to SARS-CoV-2 infection in an epicentre of the French COVID-19 epidemic: a time-series analysis. *Lancet Child Adolesc Health* 2020; published online July 2. [https://doi.org/10.1016/S2352-4642\(20\)30175-9](https://doi.org/10.1016/S2352-4642(20)30175-9).
- Grimaud M, Starck J, Levy M, et al. Acute myocarditis and multisystem inflammatory emerging disease following SARS-CoV-2 infection in critically ill children. *Ann Intensive Care* 2020; 10: 69.
- Toubiana J, Poirault C, Corsia A, et al. Kawasaki-like multisystem inflammatory syndrome in children during the covid-19 pandemic in Paris, France: prospective observational study. *BMJ* 2020; 369: m2094.
- Whittaker E, Bamford A, Kenny J, et al. Clinical characteristics of 58 children with a pediatric inflammatory multisystem syndrome temporally associated with SARS-CoV-2. *JAMA* 2020; published online June 8. <https://doi.org/10.1001/jama.2020.10369>.
- Belhadjer Z, Méot M, Bajolle F, et al. Acute heart failure in multisystem inflammatory syndrome in children in the context of global SARS-CoV-2 pandemic. *Circulation* 2020; 142: 429–36.
- Feldstein LR, Rose EB, Horwitz SM, et al. Multisystem inflammatory syndrome in US children and adolescents. *N Engl J Med* 2020; 383: 334–46.

- 11 Sanna G, Serrau G, Bassareo PP, Neroni P, Fanos V, Marcialis MA. Children's heart and COVID-19: up-to-date evidence in the form of a systematic review. *Eur J Pediatr* 2020; **179**: 1079–87.
- 12 Escher F, Pietsch H, Aleshcheva G, et al. Detection of viral SARS-CoV-2 genomes and histopathological changes in endomyocardial biopsies. *ESC Heart Fail* 2020; published online June 12. <https://doi.org/10.1002/ehf2.12805>.
- 13 Tavazzi G, Pellegrini C, Maurelli M, et al. Myocardial localization of coronavirus in COVID-19 cardiogenic shock. *Eur J Heart Fail* 2020; **22**: 911–15.
- 14 Gnechi M, Moretti F, Bassi EM, et al. Myocarditis in a 16-year-old boy positive for SARS-CoV-2. *Lancet* 2020; **395**: e116.
- 15 Craver R, Huber S, Sandomirsky M, McKenna D, Schieffelin J, Finger L. Fatal eosinophilic myocarditis in a healthy 17-year-old male with severe acute respiratory syndrome coronavirus 2 (SARS-CoV-2). *Fetal Pediatr Pathol* 2020; **39**: 263–68.

© 2020 Elsevier Ltd. All rights reserved.